Available online at www.sciencedirect.com
SCIENCE DIRECT®
Polymer 44 (2003) 6689–6696
polymer
www.elsevier.com/locate/polymer

Effects of secondary structure on miscibility and properties of semi-IPN from polyurethane and benzyl konjac glucomannan

Yongshang Lu, Lina Zhang*, Xufeng Zhang, Yan Zhou

Department of Chemistry, Wuhan University, Wuhan 430072, People's Republic of China

Received 28 February 2003; received in revised form 9 June 2003; accepted 24 June 2003

Abstract

Weight-average molecular weight (M_w) and intrinsic viscosity [η] of six fractions for benzyl konjac glucomannan (B-KGM) were determined by laser light scattering and viscometry, and the Mark–Houwink equation was established to be $[\eta] = 2.08 \times 10^{-3}\ M_w^{0.87}(cm^3\ g^{-1})$ in the M_w range of from 4.42×10^4 to 33.74×10^4 in *N*,*N*-dimethylformamide (DMF) at 25 °C. Based on current theories for a wormlike chain, the conformational parameters of B-KGM were found to be 1284 nm^{-1} for molar mass per unit contour length (M_L), 9.7 nm for persistence length (q), and 22.2 for characteristic ratio (C_∞), suggesting that B-KGM existed as a semi-stiff chain with relatively large steric-hindrance in DMF. By incorporating the semi-stiff B-KGM of different M_w into castor oil-based polyurethane, a series of semi-interpenetrating polymer networks (semi-IPN) films, coded as UB, were successfully prepared. The effects of M_w and chain conformation of B-KGM on miscibility and properties of the resulting UB films were investigated by using Fourier transform infrared spectroscopy, dynamic mechanical thermal analysis, ultraviolet spectrophotometer, and measurements of crosslink density and mechanical properties. The results indicated that the light transmittance of the UB films increased from 77 to 89% with a decrease of B-KGM M_w from 33.74×10^4 to 4.42×10^4 due to intimately interfacial adhesion between the two phases. As the B-KGM M_w decreased, the tensile strength of the UB films decreased from 15 to 5.4 MPa, whereas the elongation at break increased from 54 to 120%, resulted from that the stiff B-KGM molecules of lower M_w could easily penetrated into PU phase to hinder the formation of PU network. Miscibility between PU and lower M_w B-KGM was obviously higher than that between PU and higher M_w B-KGM, due to the relatively large specific surface provided by lower M_w B-KGM similar to 'nanoparticle'. Meanwhile, miscibility between PU and B-KGM was higher than that between PU and nitrocellulose or nitro-KGM, indicating that the effect of the chain stiffness of the natural polymers on the miscibility of the semi -IPN systems not be negligible.

Keywords: Molecular weight; Chain stiff; Miscibility

1. Introduction

It is well known that the secondary structure such as molecular weight and chain conformation is one of most important factors governing the process and application for polymers. However, the effect of the weight-average molecular weight (M_w) on polymer structure and properties is a very complicated issue, and there are few generally applicable-theoretical predications [1]. It is reported that the M_w could determine the polymer properties, such as rheological characteristics [2,3], mechanical stiffness and toughness [3,4] and miscibility between two polymers, like that of polystyrene (PS)/poly(α-methylstyrene) (PαMS) blends [5–9]. In our laboratory, the semi-interpenetrating polymer networks (semi-IPN) materials of polyurethane (PU)/nitro-cellulose (NC) [10] and PU/nitro-konjac glucomannan (NKGM) [11], exhibiting excellent properties, have been prepared. The experimental results showed that the lower M_w NC or NKGM could blend more easily with PU than the higher M_w one. It is worth noting that the content of NC or NKGM was less than 30 wt% in the semi-IPN films. Otherwise, the preparation difficulty or poor properties would result. The IPN system provided an effective way for modification and exploitation of natural polymers such as polysaccharides and protein from renewable resources. Therefore, a basic understanding of the relationship of molecular size and shape for the natural polymers with the miscibility and properties of the resulting composite

* Corresponding author. Tel.: +86-27-87219274; fax: +86-27-87882661.
E-mail address: lzhang@public.wh.hb.cn (L. Zhang).

0032-3861/03/$ - see front matter © 2003 Published by Elsevier Ltd.
doi:10.1016/S0032-3861(03)00594-9

materials is essential for their successful researches and applications. However, the effects of molecular weight and chain conformation of natural polymers on the structure and physical properties of the semi-IPN materials have not been enough investigated.

Konjac glucomannan (KGM), a polysaccharide obtained from the tubers of the *Amorphophallus konjac* plants, is a random copolymer composed of (1 → 4) linked β-D-mannose and β-D-glucose units with 10 branch points for every 32 repeating units of the main-chain [12–14]. In our previous work [15], the benzyl konjac glucomannan (B-KGM) was prepared by reacting benzyl chloride with KGM in their aqueous solution, and then used to prepare a series of castor-oil based PU/B-KGM semi-IPN films. Interestingly, the films were miscible on the molecular level or partially miscible in the range of B-KGM content from 5 to 80 wt% and exhibited morphological transition from predominated PU phase to predominated B-KGM phase, resulting in the transition of mechanical properties from highly extensible elastomers to toughened plastics. In order to know why the miscibility between PU and B-KGM was much better than that between PU and NC [10] or nitro-KGM [11], we, in this work, attempt to clarify the effects of M_w and chain conformation of B-KGM on morphology, miscibility and properties of the PU/B-KGM semi-IPN materials. The M_w and intrinsic viscosity $[\eta]$ of the six fractions of B-KGM in *N*,*N*-dimethylformamide were determined by light scattering and viscometry, and molecular parameters and chain conformation were evaluated based on current theories for a wormlike chain. Then, the semi-IPN films from PU and B-KGM were prepared, and investigated by FT-infrared spectroscopy (FT-IR), dynamic mechanical analysis (DMA), ultraviolet spectrophotometer, and the measurements of swelling and mechanical properties.

2. Experimental

2.1. Materials

All the chemical reagents used here were obtained from commercial resources in China. The chemical pure castor oil was dehydrated at 100 °C under 20 mmHg for 1 h. 2,4-Toluene diisocyanate (TDI) was redistilled before use. *N*,*N*-Dimethylformamide (DMF) was dried over molecular sieves before use. Purified KGM was supplied by Zhuxi Konjac Institute of Hubei province, China. The other reagents were used without further purification.

2.2. Preparation of B-KGM fractions

Five grams KGM was dissolved in 200 ml water, after that, the HCl was introduced and HCl concentration was adjusted to 10 wt%. The resulting mixing solution was stirred for desired time to degrade KGM. Subsequently, the apparent pH of the mixture solution was adjusted to 7 using 40 wt% NaOH aqueous solution, and the solution was introduced to a three-necked flask equipped with a mechanical stirrer, dropping funnel and condenser. The solution contained in the flask was stirred vigorously at 40 °C, while 50 g of 40 wt% NaOH aqueous solution was added dropwise. The resulting alkali-KGM slurry was stirred at 40 °C for 1 h before adding dropwise 15 g of benzyl chloride. The reaction was performed at 100 °C for 2 h, after which the slightly yellow precipitate was distilled with water-vapor, extracted with ethanol, washed with ether and water, finally, vacuum-dried at room temperature to obtain a white powder of the B-KGM. By adjusting degradation time of B-KGM in HCl aqueous solution for 1, 2, 3, 5 and 7 h, a series of B-KGM factions with different M_w was obtained and coded, respectively, as B-KGM-1, B-KGM-2, B-KGM-3, B-KGM-5 and B-KGM-7. The B-KGM prepared without the degradation was coded as B-KGM-0.

2.3. Preparation of PU/B-KGM semi-IPN

The castor oil-based PU prepolymer (NCO/OH = 2) was prepared according to the method described by Sperling et al. [16]. Three grams PU prepolymer, 20 wt% B-KGM and 1,4-butanediol as chain extender (to give total NCO/OH = 1.0) were dissolved in DMF to give a solid content of 20 wt%. The mixture solution was poured into a mould after stirred for 30 min. The casting solution was cured at room temperature for 30 min, and then heated at 60 °C for 4 h to form PU/B-KGM semi-IPN film with thickness of 150 μm. The resulting films were coded, respectively, as UB-0, UB-1, UB-2, UB-3, UB-5 and UB-7, corresponding to the B-KGM degradation time from 0 to 7 h.

2.4. Viscosity and molecular weight measurements

The $[\eta]$ values of the B-KGM fractions in DMF were determined by using an Ubbelohde viscometer at 25 ± 0.2 °C. The Huggins and Kraemer equations were used to estimate $[\eta]$ as follows:

$$\eta_{sp}/c = [\eta] + k'[\eta]^2 c \quad (1)$$

$$(\ln \eta_r)/c = [\eta] - k''[\eta]^2 c \quad (2)$$

where k' and k'' are constants for a given polymer at given temperature in a given solvent; η_{sp}/c, the reduced specific viscosity; $(\ln \eta_r)/c$, the inherent viscosity.

The M_w values of the B-KGM fractions in dimethylsulfoxide (DMSO) were determined by using static multiangle laser light scattering instrument equipped with a He–Ne laser ($\lambda = 632.8$ nm) (DAWN-DSP, Wyatt Technology Co., USA) in the angle range from 42° to 136° at 25 °C. Refractive index increment (d*n*/d*c*) was measured with a double-beam-differential refractometer (DRM-1020, Otsuka Electronic Co., Japan) at 632.8nmnm at 25 °C. All solutions were filtered with a sand filter, and then with 0.45 μm filter (DTFE, Puradisc™ 13 mm Syringe Filter,

Whattman, England). Astra software was utilized for the data acquisition and analysis.

2.5. Characterization

The FT-IR spectra of the B-KGM and UB films were recorded with a spectrometer (1600, Perkin–Elmer Co., USA) using KBr-pellets at room temperature. The degree of substitution (DS) was calculated from elemental data obtained by using an elemental analyzer (CHN-O-RAPID Heraeus Co., Germany) according to Ref. [17].

Dynamic mechanical analysis (DMA) was carried out on a dynamic mechanical thermal analyzer (DMTA-V, Rheometric Scientific Co., USA) at 1 Hz and a heating rate of 5 °C/min in the temperature range from −50 to 200 °C. The specimens with typical size of 10 mm × 10 mm (length × width) were used.

The percent light transmittance of the films was measured by using an ultraviolet spectrophotometer (UV-160A, Shimadzu, Japan). The tensile strength (σ_b) and elongation at break (ϵ_b) of the films were carried out on an universal testing machine (CMT6503, Shenzhen SANS test machine Co. Ltd., China) at a tensile speed of 10 mm/min, and an average value of at least five replicates of each material was taken.

2.6. Swelling test

The crosslink density of the various UB films was determined by swelling tests. Prior to the testing, the UB films were extracted with acetone to free the soluble material. Three film samples having weight of approximately 0.2 g each were placed into toluene and allowed to stand for 5 days at 25 °C. After swelling equilibrium, the resulting samples were removed from the toluene and weighted after removing excess toluene. The crosslink density of the UB films was obtained by using the following equation:

$$\frac{\nu_c}{V_0}(\text{mol/cm}^3) = \frac{-2[\upsilon + \chi\upsilon^2 + \ln(1-\upsilon)]}{V_1(2\upsilon^{1/3} - \upsilon)} \quad (3)$$

where ν_c = effective molar number of crosslinked chains, V_1 = molar volume of solvent, χ = polymer–solvent interaction parameter, υ = volume fraction of dry polymer in swollen gel ($\upsilon = V_0/V$), V_0 = volume of dry polymer; V = volume of swollen gel at equilibrium.

In order to determine χ of the PU/B-KGM semi-IPN in toluene system, the swelling tests were performed at 27, 29, 32 and 36 °C. From the temperature dependency of the swelling volume, χ values were obtained as following [18]

$$\frac{\mathrm{d}\ln\upsilon}{\mathrm{d}\ln T} = \frac{-3\chi(1-\upsilon)}{5(1-\chi)} \quad (4)$$

where T is temperature (K). χ values of the UB films were obtained to be from 0.34 to 0.37, here, the mean value of 0.35 for the UB films was used to calculate the crosslink density. The density of the UB films at 27, 29, 32 and 36 °C were measured by determining the weight of a volume-calibrated pycnometer filled with a mixture of NaCl aqueous solution and ethanol, in which the sample achieved floatation level.

3. Results and discussion

3.1. Molecular weight and chain conformation of B-KGM

The data of M_w, $[\eta]$ and degree of substitution (DS) for six B-KGM fractions are summarized in Table 1. The results indicated that the M_w and $[\eta]$ of the B-KGM fractions decreased with an increase of the degradation time, and the M_w values ranged from 4.42×10^4 to 33.7×10^4. The $[\eta]$ of B-KGM in DMF was much higher than that of the general vinyl polymers with same M_w, such as polystyrene and polymethacrylate, implying that the chain of B-KGM was more extended in DMF. The DS values range from 1.1 to 1.3, suggesting that the effect of DS on the chain conformation can be neglected here. Therefore, the conformation parameters of the B-KGM can be estimated according to the current theories of the solution properties. The M_w dependence of $[\eta]$ for B-KGM in DMF at 25 °C is plotted in Fig. 1. The data point for B-KGM displayed upward deviation at $\log M_w = 4.70$. This point is neglected, the Mark–Houwink equation for B-KGM in DMF in the M_w range from 8.96×10^4 to 33.74×10^4 was established to be

$$[\eta] = 2.08 \times 10^{-3} M_w^{0.87}(\text{cm}^3\ \text{g}^{-1}) \quad (5)$$

The exponent value (α) is related to the shape of the macromolecules and the nature of the solvent. The α of 0.87 suggests that the chain of B-KGM molecule was relatively expanded in DMF. Bushin [19] and Bohdaneckỳ [20] independently showed that the Yomakawa–Fujii–Yoshizaki (YFY) equation [21,22] for $[\eta]$ of the

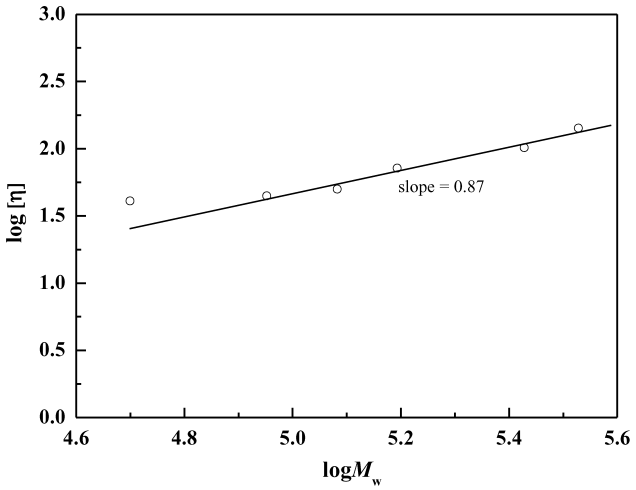

Fig. 1. M_w dependence of intrinsic viscosity ($[\eta]$) for B-KGM in DMF at 25 °C.

Table 1
The data of M_w, ([η]) and degree of substitute (DS) for B-KGM

B-KGM	B-KGM-0	B-KGM-1	B-KGM-2	B-KGM-3	B-KGM-5	B-KGM-7
$M_w \times 10^{-4}$	33.7	26.7	15.8	12.1	8.96	4.42
[η] ($cm^3\ g^{-1}$)	141.9	101.7	67.5	50.1	44.5	31.9
DS	1.1	1.2	1.2	1.1	1.3	1.2

unperturbed wormlike cylinder can be replaced approximately by

$$(M^2/[\eta])^{1/3} = A_\eta + B_\eta M^{1/2} \quad (6)$$

$$A_\eta = A_0 M_L \Phi_{0,\infty}^{-1/3} (g^{1/3}\ cm^{-1}) \quad (7)$$

$$B_\eta = B_0 \Phi_{0,\infty}^{-1/3} (2q/M_L)^{-1/2} (g^{1/3}\ cm^{-1}) \quad (8)$$

where A_0 and B_0 are tabulated in Bohdaneckỳ's paper [20], q and M_L are the persistence length and the molar mass per unit contour length, respectively. $\Phi_{0,\infty} = 2.87 \times 10^{23}$. Molecular parameters of the polysaccharides and their derivatives, such as cellulose trinitrate [20], cellulose diacetate [23], schizophyllan [24] and xanthan [25], have been successfully evaluated by using YFY equation. The B-KGM is also a polysaccharide derivative with side groups similar to the structure of polymers mentioned above. Therefore, the molecular parameters of B-KGM can also be calculated with YFY theory. The plot of $(M^2/[\eta])^{1/3}$ vs $M^{1/2}$ for B-KGM in DMF is presented in Fig. 2. By neglecting the data point of $M_w^{1/2} = 2.16$ due to downward derivation similar to Fig. 1, the values of A_η and B_η were obtained to be 203.3 and 1.283, respectively. Both A_0 and B_0 are function of the chain diameter d relative to $2q$, the relations can be described by Eqs. (9)–(11) [20]:

$$d_r^2/A_0 = (4\Phi_{0,\infty}/1.215\pi N_A)(\upsilon/A_\eta)B_\eta^4 \quad (9)$$

$$\log(d_r^2/A_0) = 0.173 + 2.158 \log d_r (d_r \leq 0.1) \quad (10)$$

$$d_r = d/2q \quad (11)$$

where υ is the partial specific volume of the polymer

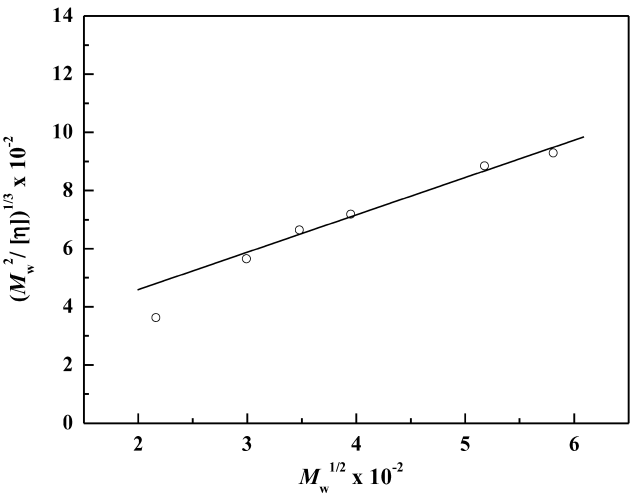

Fig. 2. The plot of $(M_w^2/[\eta])^{1/3}$ vs $M_w^{1/2}$ for B-KGM in DMF at 25 °C.

molecules, $N_A = 6.02 \times 10^{23}$. Substitution of the above A_η and B_η values together with the d_r value of 0.0791 evaluated by an alternative way in equations from (7), (8) and (11) yields 1.53 nm for d, 1284 nm^{-1} for M_L and 9.71 nm for q. This is indicative of characteristic of a semi-stiff chain. That is to say, the chain of B-KGM was relatively extended in DMF. The characteristic ratio (C_∞) can represent how much the chain is extended by steric hindrance. The C_∞ can be defined as follows [26]:

$$C_\infty = M_0/(\lambda M_L l^2) \quad (12)$$

where M_0 is the molar mass of the B-KGM repeat unit. λ^{-1} is the Kuhn's segment length, and l is the virtual bond length, which equals to the distance between two successive monosaccharidic oxygen atoms O(1) and O′(4) in the present case. By combining 0.50 nm for l of B-KGM calculated from an arithmetical average of β-(1 → 4)-D-glucan (0.425 nm) and β-(1 → 4)-D-mannoses (0.54 nm) [28] with $M_0 = 370$, $\lambda^{-1} = 19.4$ nm and $M_L = 1284\ nm^{-1}$, the C_∞ of the B-KGM in DMF was calculated to be 22.2. The C_∞ values of the general derivatives of cellulose and polysaccharides range from 10 to 17, such as 12.6 of guar galactomannan, a slightly stiffened random-coil chain in aqueous solution, consisted of a β-(1 → 4)-D-mannopyranosyl backbone partially substituted at O-6 with a galactopyranosyl side-groups [27]. Usually, the C_∞ of polymers is affected by bond angle and steric hindrance including backbone chain and side chain, etc. In this case, the relatively large C_∞ of B-KGM may be attributed to a larger steric-hindrance caused by relatively large benzyl groups linked to the backbone. Therefore, the B-KGM molecules existed as a semi-stiff chain with a relatively large steric hinderance in DMF solution.

3.2. Effects of molecular weight and chain stiffness on miscibility

The dependence of crosslink densities (v_c/V_0) on B-KGM M_w for the UB films is shown in Fig. 3. As the M_w of B-KGM decreased from 33.74×10^4 to 4.42×10^4, the crosslink densities of the resulting UB films decreased from 2.37×10^3 to 1.53×10^3 mol cm^{-3}. This can be explained as the semi-stiff B-KGM of lower M_w hindered the formation of PU networks more easily than that of higher M_w. Yoshida et al. [28] have reported that the crosslink density of the PU, consisting of polymeric MDI, propylene oxide-based polyether triol and kraft lignin fraction with different molecular weights, increased with

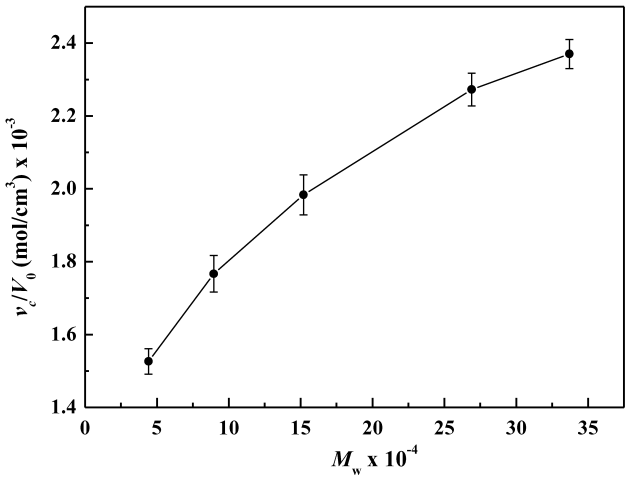

Fig. 3. The dependence of crosslink density (v_c/V_0) on B-KGM M_w for the UB films.

an increase of lignin M_w, because of the increase in functionality of the kraft lignin with higher M_w. This was different from the present PU/B-KGM semi-IPN system, in which the reaction ability of NCO groups in PU with remaining OH groups in B-KGM was nearly neglected [15]. Therefore, the results in this case may be related to the difference in the 'penetration ability' of B-KGM into PU phase. The semi-stiff B-KGM of lower M_w could more easily penetrate into the PU phase and mixed with PU than higher M_w ones to hinder the formation of PU networks [29,30]. In addition, since the B-KGM content in the UB films was kept constantly at 20 wt%, the actual semi-stiff B-KGM molecular numbers increased with a decrease of B-KGM M_w. Thus, the decreased crosslink density of the UB films could also be partially attributed to the increased B-KGM molecular number, which can effectively restrain the formation of PU networks.

It is well known that the IR spectrum can reflect the information of hydrogen bonding in polymer systems. Due to the different degree of carbonyl hydrogen bonding, the amide-I IR spectra consisted of three distinct spectral features were located at 1699–1706 cm^{-1} (hydrogen-bonded C═O groups in order domains), 1714–1719 cm^{-1} (hydrogen-bonded C═O groups in disorder domains) and 1730–1735 cm^{-1}(free C═O groups), respectively, [31–33]. FT-IR spectra of the urethane carbonyl region for the UB films are shown in Fig. 4. There were distinct differences in position and intensity of three characteristic peaks located at about 1731, 1713, and 1702 cm^{-1} for the C═O band, depending on the B-KGM M_w. Compared with that of the hydrogen bonded C═O, the relative intensity of free C═O band increased when M_w of B-KGM decreased from 33.7×10^4 to 4.42×10^4. Therefore, the free –C═O fraction in UB films having lower M_w B-KGM was more abundant than that of the UB films having higher M_w B-KGM, resulted from the disruption of hydrogen bonding between –C═O and –NH involved in hard–soft segments and hard–hard segments of PU. This can be explained that

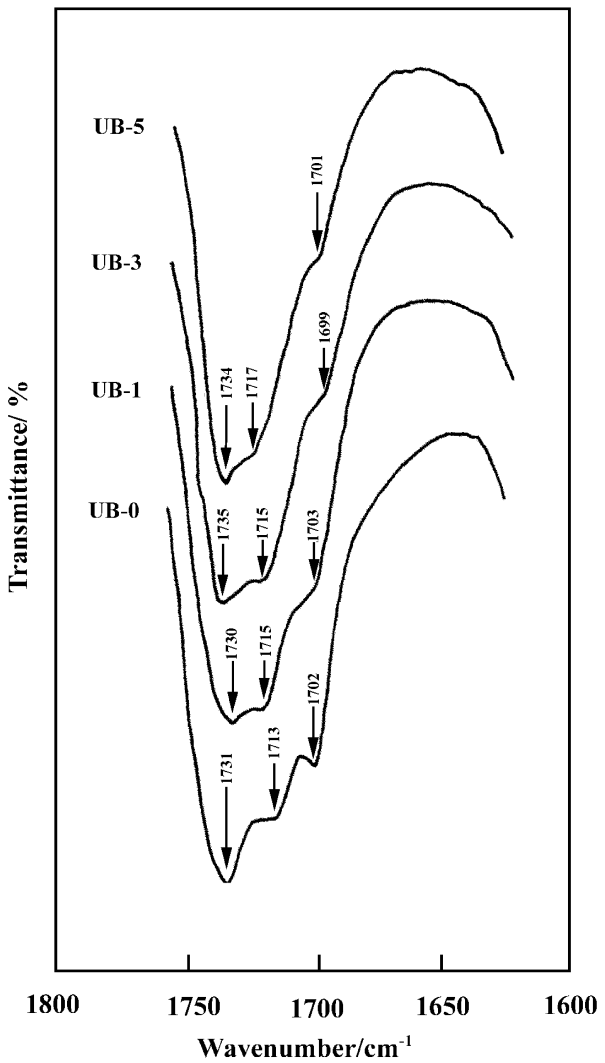

Fig. 4. FT-IR spectra of the urethane carbonyl region for the UB films.

B-KGM with the lower M_w can more easily penetrate into PU and mix with PU, resulting in the perturbation of hydrogen bonding interactions in PU itself.

The temperature dependence of storage modulus (E') for the UB films is shown in Fig. 5. When B-KGM M_w was higher than 8.96×10^4, the E' curves of the UB films exhibited two distinctive drops in stiffness at lower and higher temperature, assigned to the glass transitions (T_g) of PU and B-KGM, respectively. However, the E' of UB-7 steadily decreased until it reached the rubbery modulus, indicating a higher degree of phase mixing between PU and lower M_w B-KGM. Temperature dependence of mechanical loss factor (tan δ) for the UB films is shown in Fig. 6, and the T_g data taken from the tan δ maximum are summarized in Table 2. The T_g transition of PU was observed at about 25 °C [15]. Whereas the T_g transition of pure B-KGM was found to increase from 112 to 168 °C with the increase of B-KGM M_w from 4.42×10^4 to 33.74×10^4(shown in Table 2). The UB films exhibited two separate tan δ peaks for each phase except for the UB-7. This is indicative of micro-phase

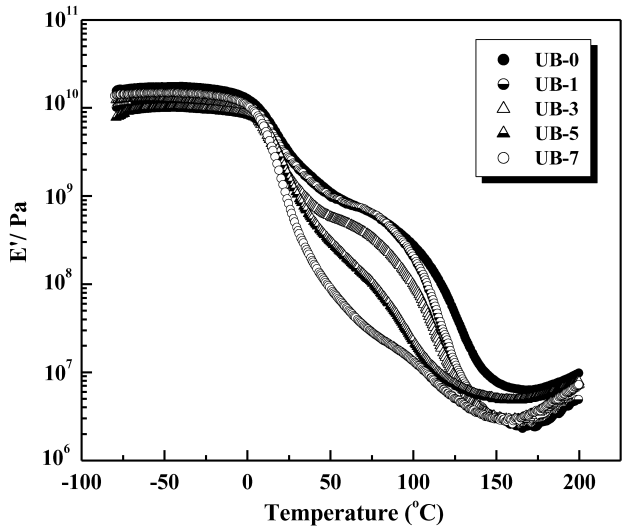

Fig. 5. Temperature dependence of storage modulus (E') for the UB films.

separation between PU and B-KGM. The T_g values of the films UB-0–UB-3, corresponding to PU, were lower than that of pure PU, owing to the loose network caused by incorporation of B-KGM. The freedom of molecular motion can be reflected by the sharpness and height of the tan δ peak [34]. The height of tan δ peaks of the UB films, corresponding to T_g transition of PU, increased with a decrease of B-KGM M_w. This can be explained by plasticization effect and, more importantly, by an incompetently formed PU networks containing defects such as loose chain ends caused by lower M_w B-KGM [30]. As the B-KGM M_w decreased, the tan δ peak, corresponding to T_g transition of B-KGM, shifted to lower temperature, broadened and flattened until it became a slight shoulder in UB-7 film, indicating an increase in miscibility between PU and lower M_w B-KGM.

It should be noted that the resulting UB films have good miscibility or certain degree of miscibility when the B-KGM content range from 5 to 80 wt% in the PU/B-KGM semi-IPN system [15], but in the previous works in our laboratory, the PU/NKGM [11] and PU/NC [10] semi-IPN films were miscible or partial miscible only when PU content was more than 70 wt%. This can be explained that B-KGM was more expanded than NC or NKGM in solution. Thus, the expanded B-KGM molecules penetrated easily into PU phase and gave larger specific surface to contact with PU. For the resulting UB films, the role of low M_w B-KGM was similar to that of nanoparticles having relatively large specific surface. The large amount of 'nanoparticles' contained in the UB films could actively interact with PU, leading to an increase in miscibility between PU and lower M_w B-KGM.

Table 2
The DMA data of PU, UB and B-KGM samples

Films	UB-0	UB-1	UB-3	UB-5	UB-7
T_g (°C) (PU)	25				
T_{g1} (°C)	14.5	16.2	16.7	24.2	26.5
T_{g2} (°C)	128.3	125.6	115.4	95.8	–
T_g (°C) (B-KGM)	168.3	156.7	141.5	129.2	112.4

T_{g1}, corresponding to T_g of PU; T_{g2}, corresponding to T_g of B-KGM.

The light transmittance (T_r) measurements are often used as an empirical method for determining the phase mixing in polymer composite materials [35]. The dependence of light transmittance (T_r) at 800 nm on B-KGM M_w for the UB films is shown in Fig. 7. Interestingly, the T_r values of the UB films increased from 75 to 89% with the decrease of B-KGM M_w. When M_w of B-KGM was lower than 15.6×10^4, the T_r values of the films UB-3, UB-5 and UB-7 were higher than that of PU. Generally, the enhanced T_r of the polymer blends may be correlative with the interfacial interactions, amorphous state, phase domain sizes as well as the match of refractive indices of the polymer components. The higher T_r

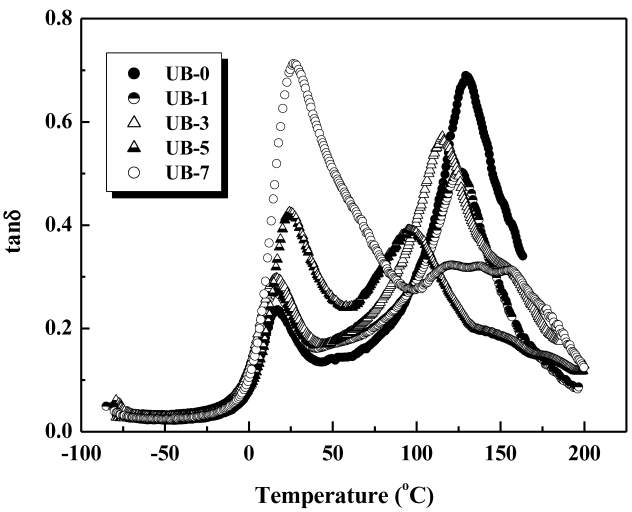

Fig. 6. Temperature dependence of mechanical loss factor (tan δ) for the UB films.

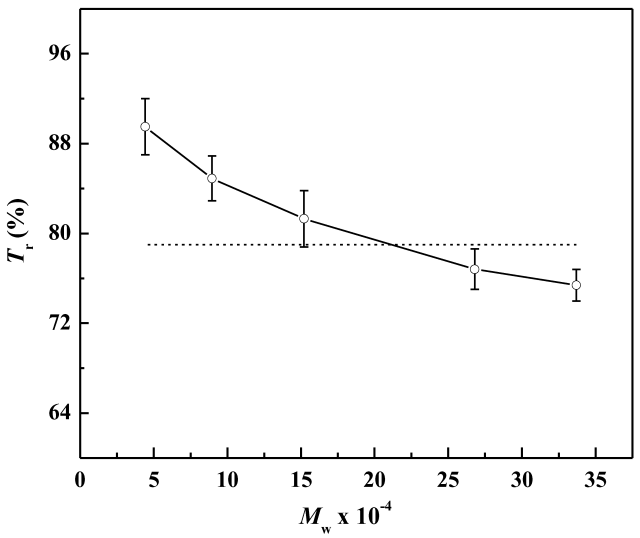

Fig. 7. The dependence of light transmittance (T_r) on B-KGM M_w for the UB films (----- represent T_r of PU).

values of the UB films imply the occurrence of the strong interaction between lower M_w B-KGM and PU matrix, resulting in the enhancement of miscibility [10,11,36].

3.3. Effects of molecular weight on mechanical properties

The dependence of tensile strength (σ_b) and elongation at break (ϵ_b) on M_w for B-KGM is shown in Fig. 8. With an increase of M_w from 4.42×10^4 to 33.7×10^4, the σ_b values of the B-KGM films increased from 39 to 57 MPa, whereas that of ϵ_b decreased from 34 to 16%. The B-KGM M_w dependence of σ_b and ϵ_b of the UB films is shown in Fig. 9. The values of σ_b and ϵ_b of the PU film were 7 MPa and 250%, respectively. As the M_w of B-KGM increased, the σ_b values of the UB films increased, and were higher than that of PU film except for that of UB-7 film. The UB-7 film exhibited lower σ_b than PU film, due to loose networks caused by incorporating of lower M_w B-KGM. The ϵ_b values of the UB films significantly increased from 54 to 122% with the decrease of B-KGM M_w, owing to the easiness of molecular motion in loose networks [37]. This is well consistent with the modulus behaviors of the UB films shown in Fig. 5. Therefore, the relatively low M_w B-KGM plays an important role in plasticizing the UB films and enhancing miscibility between PU and B-KGM.

4. Conclusions

The Mark–Houwink equation for the B-KGM in DMF solution at 25 °C was established to be $[\eta] = 2.08 \times 10^{-3} M_w^{0.87}$ ($cm^3\ g^{-1}$). Analysis of experimental data in terms of the theories for wormlike chain gave the conformational parameters of the B-KGM in DMF to be 1284 nm^{-1} for M_L, 9.7 nm for q, and 22.2 for C_∞, indicating a semi-stiff B-KGM chain with relatively large steric-hindrance exists in DMF. The semi-IPN films were prepared from castor oil-based PU and 20 wt% B-KGM with different M_w from

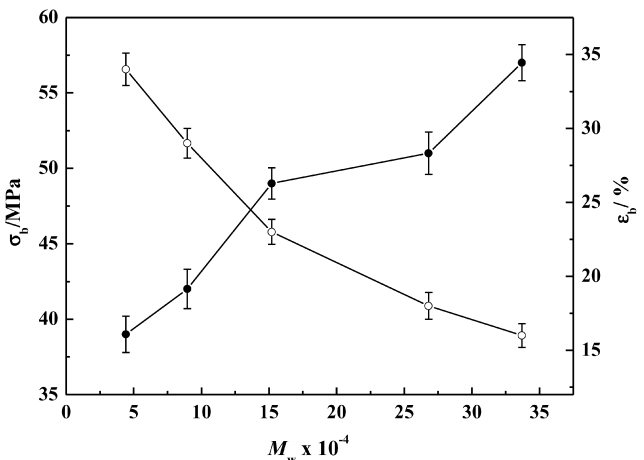

Fig. 8. The dependence of tensile strength (σ_b, ●) and elongation at break (ϵ_b, ○) on M_w for B-KGM.

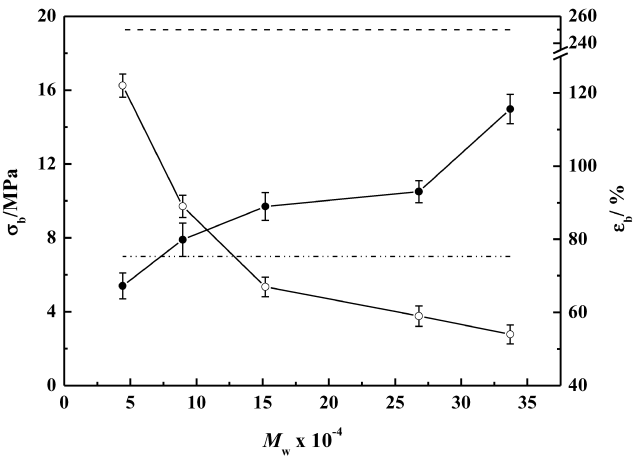

Fig. 9. The dependence of tensile strength (σ_b, ●) and elongation at break (ϵ_b, ○) on B-KGM M_w for the UB films (Marks –··–··–·· and – – – represent the σ_b and ϵ_b of the PU film, respectively).

4.42×10^4 to 33.7×10^4. The results showed that the miscibility between PU and B-KGM was much higher than that between PU and nitro-polysaccharide derivates, such as NC [10] and NKGM [11], indicating that the effect of the B-KGM chain stiffness in the semi-IPN systems could not be negligible. As the B-KGM M_w decreased, the miscibility of the UB films increased, due to the strong interaction and effective mixing between phases. The σ_b values of the UB films decreased from 15 to 5.4 MPa, but the ϵ_b values increased from 54 to 122% with the decrease of the B-KGM M_w from 33.7×10^4 to 4.42×10^4, suggesting that B-KGM of lower M_w penetrated more easily into the PU networks and hindered the formation of PU networks than the one of higher M_w. Both chain stiffness and the relatively low M_w of B-KGM play an important role in enhancing the miscibility and interaction between PU and B-KGM, similar to that of 'nanoparticle'.

Acknowledgements

This work was supported by Major Grant of the National Natural Science Foundation of China (59933070), Major Grant of Science and Technology project from Hubei Province and the Key Laboratory of Cellulose and Lignocellulosic Chemistry of The Chinese Academy of Sciences.

References

[1] Luo S, Grubb DT, Netravli AN. Polymer 2002;43:4159.
[2] Ajroldi G, Marchionni G, Pezzin G. Polymer 1999;40:4163.
[3] Nicholson LM, Whitley KS, Gates TS. Int J Fatigue 2002;24:185.
[4] Fornes TD, Yoon PJ, Keskkula H, Paul DR. Polymer 2001;42:9929.
[5] Dunn DJ, Krause S. J Polym Sci Part C: Polym Lett 1974;12:591.
[6] Lau SF, Pathak J, Wunderlich B. Macromolecules 1982;15:1278.
[7] Saeki S, Cowie JMC, McEwen IJ. Polymer 1983;24:60.
[8] Schneider HA, Dilger P. Polym Bull 1989;21:265.

[9] Windmaier JM. Macromolecles 1991;24:4209.
[10] Zhang L, Zhou Q. J Polym Sci: Polym Phys 1999;37:1623.
[11] Gao S, Zhang L. Macromolecules 2001;34:2202.
[12] Maeda M, Shimahara H, Sngiyama N. Agric Bio Chem 1980;44:245.
[13] Smith F, Strvastava HC. J Am Chem Soc 1959;81:1715.
[14] Kato K, Matsuda K. Agric Biol Chem 1973;37:2045.
[15] Lu Y, Zhang L. Polymer 2002;34:3979.
[16] Devia N, Manson JA, Sperling LH, Conde A. Macromolecules 1979; 12:360.
[17] Sugiyama N, Shimahara H, Andoh T, Takemoto M, Kamata T. Agric Biol Chem 1972;36:1381.
[18] Flory PJ, Rehner J. J Chem Phys 1943;11:521.
[19] Bushin SV, Tsvetkov VN, Lysenko EB. Vysokomol Soedin Ser A 1981;A23:2494.
[20] Bohdaneckỳ M. Macromolecules 1983;16:1483.
[21] Yamakawa H, Fujii M. Macromolecules 1974;7:128.
[22] Yamakawa H, Yoshizaki T. Macromolecules 1980;13:633.
[23] Kawanishi H. J Chem Phys 1998;108:6014.
[24] Yanaki T, Norisuye T, Teramoto A, Fujita H. Macromolecules 1980; 13:1462.
[25] Sato T, Norisuye T, Fujita H. Macromolecules 1984;17:2696.
[26] Chen J, Zhang L, Nakamura Y, Norisuye T. Polym Bull 1998;41:471.
[27] Robinson G, Ross-Murphy SB, Morris E. Carbohydr Res 1982;107: 17.
[28] Yoshida N, Shimahara H, Andoh T, Takeyama H. J Appl Polym Sci 1990;40:1819.
[29] Hong BK, Jo WH. Polymer 2000;41:2069.
[30] Hourston DJ, Schäfer F-U. Polymer 1996;37:3521.
[31] Luo N, Wang DN, Ying SK. Polymer 1996;37:3577.
[32] Christenson CP, Harthcock MA, Meadows MD, Spell HL, Howard WL, Creswick MW, Guerra RE, Turner RB. J Polym Sci Part B: Polym Phys 1986;24:1401.
[33] Nair BR, Gregoriou VG, Hammond PT. Polymer 2000;41:2961.
[34] Son TW, Lee DW, Lim SK. Polym J 1999;31:563.
[35] Krause S. J Macromol Sci: Rev Macromol Chem 1972;7:251.
[36] Yang J, Winnik MA, Ylitalo D, DeVoe RJ. Macromolecules 1996;29: 7047.
[37] Liaw DJ. J Appl Polym Sci 1997;66:1251.